

ACS photometry of newly-discovered globular clusters in the outer halo of M31¹

A.D. Mackey², A. Huxor³, A.M.N. Ferguson², N.R. Tanvir⁴, M. Irwin⁵, R. Ibata⁶, T. Bridges⁷, R.A. Johnson⁸, G. Lewis⁹

ABSTRACT

We report the first results from deep ACS imaging of ten classical globular clusters in the far outer regions ($15 \lesssim R_p \lesssim 100$ kpc) of M31. Eight of the clusters, including two of the most remote M31 globular clusters presently known, are described for the first time. Our F606W, F814W colour-magnitude diagrams extend ~ 3 magnitudes below the horizontal branch and clearly demonstrate that the majority of these objects are old ($\gtrsim 10$ Gyr), metal-poor clusters. Five have $[\text{Fe}/\text{H}] \sim -2.1$, while an additional four have $-1.9 \lesssim [\text{Fe}/\text{H}] \lesssim -1.5$. The remaining object is more metal-rich, with $[\text{Fe}/\text{H}] \sim -0.70$. Several clusters exhibit the second parameter effect. Using aperture photometry, we estimate integrated luminosities and structural parameters for all clusters. Many, including all four clusters with projected radii greater than 45 kpc, are compact and very luminous, with $-8.9 \lesssim M_V \lesssim -8.3$. These four outermost clusters are thus quite unlike their Milky Way counterparts, which are typically diffuse, sub-luminous ($-6.0 \lesssim M_V \lesssim -4.7$) and more metal-rich ($-1.8 \lesssim [\text{Fe}/\text{H}] \lesssim -1.3$).

¹Based on observations made with the NASA/ESA Hubble Space Telescope, obtained at the Space Telescope Science Institute, which is operated by the Association of Universities for Research in Astronomy, Inc., under NASA contract NAS 5-26555. These observations are associated with program 10394.

²Institute for Astronomy, University of Edinburgh, Royal Observatory, Blackford Hill, Edinburgh, EH9 3HJ, UK

³Department of Physics, University of Bristol, Tyndall Avenue, Bristol, BS8 1TL, UK

⁴Department of Physics & Astronomy, University of Leicester, Leicester, LE1 7RH, UK

⁵Institute of Astronomy, University of Cambridge, Madingley Road, Cambridge, CB3 0HA, UK

⁶Observatoire de Strasbourg, 11 rue de l'Université, F-67000 Strasbourg, France

⁷Department of Physics, Queen's University, Kingston, ON, K7M 3N6, Canada

⁸Oxford Astrophysics, Denys Wilkinson Building, Keble Road, Oxford, OX1 3RH, UK

⁹Institute of Astronomy, School of Physics, A29, University of Sydney, NSW 2006, Australia

Subject headings: galaxies: individual (M31) — galaxies: halos — globular clusters: general

1. Introduction

Globular clusters observed in M31 provide the closest example of a globular cluster system belonging to a large external galaxy. Members of this system allow us to trace the star formation history, chemical evolution, kinematics, and mass distribution in different regions of M31, and are therefore vital to our developing picture of its formation and evolution. However, very few clusters have been discovered at large distances from M31, meaning that up until now we do not possess a good sample with which to probe its outer halo. Recently, as part of a major survey of the M31 halo with the Isaac Newton Telescope (see e.g., Ferguson et al. 2002) and MegaCam on the Canada-France-Hawaii Telescope (see e.g., Martin et al. 2006), a search for previously unknown globular clusters, at large projected radii (R_p) from the center of M31, has been conducted. This search has resulted in the discovery of a significant number of new clusters, with R_p between $\sim 15 - 120$ kpc (Huxor et al. 2004, 2005; Huxor 2006; Martin et al. 2006). A sample of 14 of these objects has been the subject of deep follow-up imaging using the Advanced Camera for Surveys (ACS) on board the Hubble Space Telescope (HST). Preliminary results for four members of the population of luminous, extended clusters of Huxor et al. (2005) have recently been described (Mackey et al. 2006, hereafter Paper I). In this Letter, we present results for the remaining ten clusters, and compare, for the first time, the cluster population of the outer M31 halo to that of the outer Milky Way halo.

This sample consists of classical (compact) globular clusters with projected radii distributed in the range $15 \lesssim R_p \lesssim 100$ kpc. Only two of these objects are previously recorded – the remaining eight are new discoveries. Their positions are listed in Table 1, and presented schematically in Fig. 1. Two of the newly-discovered clusters (GC5, GC10) lie at very large distances from M31: $R_p \sim 78$ and 100 kpc, respectively. These, along with the new cluster of Martin et al. (2006), which has $R_p \sim 116$ kpc, are by far the most remote members of M31’s globular cluster system found to date. Of the two previously reported clusters in our sample, one (GC4) was first described by Huxor et al. (2004) but discovered independently by Galleti et al. (2005), who labelled it B514. This object has additional separate ACS imaging (Galleti et al. 2006). The second was observed in the same field as one of our luminous, extended clusters, and appears in the catalogue of Barmby et al. (2000) (cluster 298-021).

2. Observations and data reduction

Our observations were obtained with the ACS Wide Field Channel (WFC) under HST program GO 10394 (P.I. Tanvir), at various intervals over the period 2005 May 27 – 2005 September 17. Targets were imaged three times in the F606W filter and four times in the F814W filter, with small dithers between subsequent images. Typical total integration times were 1800s in F606W and 3000s in F814W. Each cluster was placed at the centre of either chip 1 or chip 2 on the WFC, to avoid the inter-chip gap. Drizzled F606W images of two representative clusters are displayed in Fig. 1.

Details of our photometric reduction procedure are provided in Paper I. Briefly, we used the DOLPHOT software (Dolphin 2000), specifically the ACS module, to conduct PSF-fitting photometry on all images. Output measurements are on the VEGAMAG scale of Sirianni et al. (2005). We used the quality information provided by DOLPHOT to clean the resulting detection lists, selecting only stellar detections, with valid photometry on all input images, global sharpness parameter between -0.3 and 0.3 in each filter, and crowding parameter less than 0.25 in each filter. Field stars are present in all images; however, their densities are typically sparse since the clusters are at such large projected radii from M31. To eliminate field star contamination from our cluster colour-magnitude diagrams (CMDs), we imposed limiting radii from the cluster centers. Because of the sparse fields, these radii were typically quite generous ($\sim 25''$). However, two clusters (GC6, GC7) are set against heavier background fields and hence required smaller limiting radii of $10''$. From the resulting CMDs (see below), it is evident that field star contamination is not a significant issue – in all cases the principal cluster sequences are very clearly visible. Therefore, a more sophisticated statistical subtraction is not necessary at this stage.

3. Analysis

Fig. 2 shows CMDs for our ten clusters. The photometry reaches ~ 3 mag below the level of the horizontal branch (HB), to a limiting magnitude of $m_{F606W} \sim 28$. All clusters exhibit narrow red-giant branches (RGBs) and clearly delineated HBs. Nine of the clusters possess rather steep RGBs, indicating they are metal-poor objects. Many of these clusters also feature HBs extending to the blue, including broadened regions with colours in the range $0.1 \lesssim m_{F606W} - m_{F814W} \lesssim 0.5$ which are suggestive of RR Lyrae stars imaged at random phase. Such clusters are old, with ages $\gtrsim 10$ Gyr. GC7 has a noticeably different CMD from those of the other clusters, with a sharply bending RGB and very stubby red HB, characteristics indicative of a more metal-rich object.

We obtained photometric metallicity estimates using a procedure we previously described and verified in Paper I. Because our sample covers a very wide spatial area and range in R_p , we could not assume a uniform distance and reddening. Instead, we determined the best-fitting combination of $[\text{Fe}/\text{H}]$, $(m - M)_0$, and $E(B - V)$ for a given cluster by registering the ACS/WFC F606W and F814W Galactic globular cluster fiducials of Brown et al. (2005) to the appropriate CMD using the F606W level of the HB and the colour of the RGB at the HB level. A fiducial of the correct $[\text{Fe}/\text{H}]$ closely traces the upper RGB on the CMD when registered in this way, while a fiducial of incorrect $[\text{Fe}/\text{H}]$ deviates on the upper RGB. The cluster metallicity is estimated by bounding the RGB with a more metal-poor and a more metal-rich fiducial. We assume *a priori* that the main body of M31 has $(m - M)_0 = 24.47 \pm 0.07$ (McConnachie et al. 2005). For each cluster we registered fiducials using, incrementally, a range ± 0.5 mag about this value (i.e., a system depth of ~ 360 kpc). At each $(m - M)_0$ we used Brown et al.’s transformations to solve for the $E(B - V)$ which aligned the fiducial and CMD HB levels. Applying this reddening, we determined the offset between the color of the fiducial RGB at HB level and that of the cluster CMD. The best fitting combination of $(m - M)_0$ and $E(B - V)$ for a given fiducial was that which minimized this offset. To determine uncertainties in these values we randomly selected ten thousand Gaussian deviates about the two HB levels and the RGB colour at HB level (widths were typically ± 0.1 mag and ± 0.01 mag, respectively) and calculated new $E(B - V)$ and $(m - M)_0$ for each. We derived standard random errors from the resulting distributions. We note that there are possibly additional systematic errors present for our measured $E(B - V)$ values, due to differences in age between the M31 clusters and the fiducial clusters, and the fact that the colour of the RGB at the HB level is mildly age-sensitive. For the majority of clusters (with the exceptions discussed below), these errors would amount at most to ~ 0.02 mag more than quoted in Table 1, corresponding to the interval 10 – 15 Gyr.

Fig. 3 shows the fiducial registration, while numerical results are listed in Table 1. The derived metallicities reflect those adopted for the reference clusters by Brown et al. (2005). Our typical measurement uncertainties are ± 0.15 dex.

The majority of our clusters are confirmed as metal-poor objects. Five have RGBs well traced by the M92 fiducial ($[\text{Fe}/\text{H}] = -2.14$), and two have RGBs bounded by M92 and NGC 6752 ($[\text{Fe}/\text{H}] = -1.54$). Two more have RGBs matched by the NGC 6752 fiducial. The remaining cluster, GC7, is more metal-rich, with its RGB matched by 47 Tuc ($[\text{Fe}/\text{H}] = -0.70$). Two clusters have previous metallicity measurements. Galleti et al. (2006) derived, photometrically, $[\text{Fe}/\text{H}] \sim -1.8$ for GC4. GC6 has a spectroscopic measurement by Perrett et al. (2002), who found $[\text{Fe}/\text{H}] = -2.07 \pm 0.11$. Both values are in reasonable agreement with our estimates.

We also compared our derived $E(B - V)$ with those from the maps of Schlegel et al. (1998, SFD) (listed in Table 1). Agreement is adequate, although we note a tendency to derive larger $E(B - V)$ than SFD by a few hundredths of a mag – we noticed a similar effect in Paper I. Adopting the SFD values forces our $(m - M)_0$ to be greater by ~ 0.025 mag per 0.01 mag difference in $E(B - V)$; however the fiducial registration is often noticeably inferior. The discrepancy may be due to spatial reddening variations on smaller scales than resolved by the SFD maps (6'1), a systematic error introduced by slightly different ages for the M31 and template clusters (as noted above), or to a systematic error in the colour excesses adopted by Brown et al. (2005) for their reference clusters.

Most of our derived distance moduli lie close to the canonical value for M31: $(m - M)_0 = 24.47$ (~ 780 kpc). However, our measurements for GC7 and GC9 suggest these clusters may be closer by ~ 115 kpc and ~ 85 kpc, respectively. This would render GC7, in particular, an unusual object, given its $[\text{Fe}/\text{H}]$. In the Milky Way, there are two prominent globular clusters at unusually large radii for their $[\text{Fe}/\text{H}]$: Ter 7 and Pal 12. Both these clusters are only about 70% the age of the oldest Galactic globulars. If GC7 is similarly young, then fitting the Brown et al. (2005) fiducials is inappropriate. We note that the CMD of GC7 shows an overdensity of points around $m_{\text{F606W}} \sim 27.5$ and $m_{\text{F606W}} - m_{\text{F814W}} \sim 0.5$ which is not present in the other cluster CMDs. The presence of the main-sequence turn-off in this region, blurred by observational errors, could explain this bulge. If this is the case, then GC7 may be as young as ~ 4 Gyr, based on CMDs for LMC and SMC clusters. To check our measured $E(B - V)$ and $(m - M)_0$ for GC7, we transformed our photometry to Johnson-Cousins V and I (Siriani et al. 2005) and matched the fiducials of Sarajedini & Layden (1997) and Rosenberg et al. (1998) for Ter 7 and Pal 12, respectively. These objects have comparable $[\text{Fe}/\text{H}]$ to GC7. The fiducial fits result in $E(B - V) \sim 0.07$ and $(m - M)_0 \sim 24.3$, much more similar to the quantities observed for our other M31 clusters. We note that both Ter 7 and Pal 12 are unambiguously associated with the accreted Sagittarius dSph. GC7 may represent a similar scenario in M31 – verification of our measurements would therefore be valuable.

Inspection of Fig. 2 and our measured $[\text{Fe}/\text{H}]$ reveals several second parameter clusters. We defer numerical calculation of HB morphologies until a future paper when tests for completeness and photometric blends can be incorporated. Even so, the second parameter effect is clear for GC5, which has a red HB but equivalent $[\text{Fe}/\text{H}]$ to GC2, and EC1 from Paper I. Similarly, GC8 and GC9 have $[\text{Fe}/\text{H}] \sim -1.54$; however they have much redder HBs than comparable Galactic globulars (e.g., NGC 1904, 6752, 7492). The HBs of these two objects resemble those for many of the M31 clusters with similar $[\text{Fe}/\text{H}]$ but smaller R_p observed by Rich et al. (2005), and second parameter Galactic globulars such as Pal 14.

Finally, we calculated integrated cluster luminosities by means of aperture photometry centred on the cluster centres. This technique ensures all light is counted, even in the unresolved cores of the most compact objects. For a given cluster, we first estimated the sky level using regions away from the cluster, and produced a sky subtracted image. At large projected radii from M31, we do not have to worry about a significantly spatially variable background. We then masked any bright background galaxies or foreground stars in the vicinity of the cluster. Next, we measured integrated luminosities using a variety of apertures. In combination with the cluster CMDs, plotting luminosity as a function of aperture radius allowed us to check for field star contamination. For the most remote clusters, where field contamination is extremely sparse, the integrated luminosity quickly reached an asymptotic limit. For such objects a maximum radius of $20''$ was more than sufficient. For objects set against more significant fields, contamination manifested in the form of a slowly increasing integrated luminosity with increasing aperture radius (as well as being visible in the CMD). For these objects, the cluster light always dominates for radii smaller than $10''$. Beyond this, we used our plots to estimate the radius at which field star contamination became non-negligible (r_{\max}) and integrated only to this limit. Three clusters have $r_{\max} = 10''$, while the remainder have $16'' \leq r_{\max} \leq 20''$. We used our summed magnitudes in F606W and F814W to transform the F606W value to Johnson V (Sirrianni et al. 2005), and then used the relevant $E(B - V)$ and $(m - M)_0$ to calculate M_V . We next re-sampled with smaller apertures to estimate the half-light radius r_h , which we converted to parsecs using our $(m - M)_0$ values. All results are listed in Table 1. Clusters with $r_{\max} \gtrsim 16''$ have reliable M_V – as noted above, the integrations are very close to asymptotic by such radii. For the three with $r_{\max} = 10''$, we used the profiles of the clusters with negligible field contamination to observe that M_V may be under-estimated by ~ 0.1 mag. This level of uncertainty is acceptable for present purposes – it is less even than the uncertainties introduced by application of the derived distance moduli.

With our new sample of remote M31 members, we are, for the first time, in a position to compare the outer globular cluster system of this galaxy with that of our own. Doing so reveals striking differences between the two. Seven Galactic globular clusters have $R_{gc} > 40$ kpc (Pyxis; Pal 3, 4, and 14; AM-1; Eridanus; and NGC 2419). Of these, all except NGC 2419 have $-1.8 \lesssim [\text{Fe}/\text{H}] \lesssim -1.3$, and are sub-luminous ($-6.0 \lesssim M_V \lesssim -4.7$) and very extended ($11 \lesssim r_h \lesssim 25$ pc). NGC 2419 is one of the most luminous clusters in our Galaxy ($M_V \sim -9.6$), and lies in an unusual position on the luminosity vs. size plane. This has led to some suggestions it may be the remains of an accreted galaxy (e.g., van den Bergh & Mackey 2004). In our present sample, we have four M31 globulars at $R_p > 40$ kpc. In contrast with the majority of outer Milky Way clusters, these objects are very metal-poor ($-2.2 \lesssim [\text{Fe}/\text{H}] \lesssim -1.8$), compact ($4 \lesssim r_h \lesssim 7$ pc) and very bright ($-8.9 \lesssim M_V \lesssim -8.3$). Unlike

NGC 2419, none of the clusters lie in an unusual position on the luminosity vs. size plane, suggesting that they are 'normal' globular clusters. The new cluster of Martin et al. (2006), at $R_p \sim 116$ kpc is also compact and luminous ($M_V \sim -8.5$), while EC4 from Paper I, at $R_p \sim 60$ kpc, is a member of the population of luminous, extended M31 globular clusters which has no Galactic analogue.

It is perhaps not surprising that we have not observed any very extended, sub-luminous globular clusters in the remote M31 halo – such objects may well lie below our present survey detection limit. Even so, the above comparison shows that *M31 clearly possesses an extended system of metal-poor, compact, and very luminous globular clusters which is not seen in the Milky Way*. The one luminous, metal-poor outer Milky Way cluster – NGC 2419 – is quite unlike the M31 clusters we have observed (as described above). Furthermore, the outermost M31 globular clusters studied here are considerably more metal-poor than the pressure-supported field halo population at the same radii (Chapman et al. 2006; Kalirai et al. 2006), again in contrast to the Milky Way. These disparities may well offer important clues to differences in the early formation and evolution of the two galaxies or in their subsequent accretion histories, and as such, it is vital that additional M31 members are sought. We remark that the present sample has been obtained from a survey of ≈ 100 square degrees, roughly 25% of the area contained within a projected radius of 150 kpc of M31. A significant number of new clusters may therefore await detection, suggesting that, unlike in the Milky Way, there may be a relatively large population of luminous, compact globular clusters in the outer M31 halo. Such objects, in addition to their value as globular clusters, are extremely useful as dynamical probes of the mass distribution in M31 – work which has previously relied on clusters with $R_p \lesssim 25$ kpc and a handful of dwarf galaxies. We anticipate that our new sample will soon allow improved mass constraints to be determined.

ADM and AMNF are supported by a Marie Curie Excellence Grant from the European Commission under contract MCEXT-CT-2005-025869. NRT acknowledges financial support via a PPARC Senior Research Fellowship.

Facilities: HST (ACS).

REFERENCES

- Barmby, P., Huchra, J. P., Brodie, J. P., Forbes, D. A., Schroder, L. L., & Grillmair, C. J. 2000, *AJ*, 119, 727
- Brown, T. M., et al. 2005, *AJ*, 130, 1693

- Chapman, S. C., Ibata, R., Lewis, G. F., Ferguson, A. M. N., Irwin, M., McConnachie, A., & Tanvir, N. 2006, *ApJ*, in press
- Dolphin, A. E. 2000, *PASP*, 112, 1383
- Ferguson, A. M. N., Irwin, M. J., Ibata, R. A., Lewis, G. F., & Tanvir, N. R. 2002, *AJ*, 124, 1452
- Galleti, S., Bellazzini, M., Federici, L., Fusi Pecci, F. 2005, *A&A*, 436, 535
- Galleti, S., Federici, L., Bellazzini, M., Buzzoni, A., & Fusi Pecci, F. 2006, *ApJL*, in press (astro-ph/0609439)
- Huxor, A. P. 2006, Ph.D. Thesis, University of Hertfordshire
- Huxor, A., Tanvir, N., Irwin, M., Ferguson, A., Ibata, R., Lewis, G., & Bridges, T. 2004, in *ASP Conf. Ser. 327, Satellites and Tidal Streams*, ed. F. Prada, D. Martínez Delgado, & T. Mahoney (San Francisco: ASP), 118
- Huxor, A. P., Tanvir, N. R., Irwin, M. J., Ibata, R., Collett, J. L., Ferguson, A. M. N., Bridges, T., & Lewis, G. F. 2005, *MNRAS*, 360, 1007
- Kalirai, J. S., et al. 2006, *ApJ*, 648, 389
- Mackey, A. D., et al. 2006, *ApJL*, submitted (Paper I)
- Martin, N. F., Ibata, R. A., Irwin, M. J., Chapman, S., Lewis, G. F., Ferguson, A. M. N., Tanvir, N., & McConnachie, A. W. 2006, *MNRAS*, 371, 1983
- McConnachie, A. W., Irwin, M. J., Ferguson, A. M. N., Ibata, R. A., Lewis, G. F., & Tanvir, N. 2005, *MNRAS*, 356, 979
- Perrett, K. M., Bridges, T. J., Hanes, D. A., Irwin, M. J., Brodie, J. P., Carter, D., Huchra, J. P., and Watson, F. G. 2002, *AJ*, 123, 2490
- Rich, R. M., Corsi, C. E., Cacciari, C., Federici, L., Fusi Pecci, F., Djorgovski, S. G., & Freedman, W. L. 2005, *AJ*, 129, 2670
- Rosenberg, A., Saviane, I., Piotto, G., & Held, E. V. 1998, *A&A*, 339, 61
- Sarajedini, A., & Layden, A. 1997, *AJ*, 113, 264
- Schlegel, D. J., Finkbeiner, D. P., & Davis, M. 1998, *ApJ*, 500, 525 (SFD)
- Sirianni, M., et al. 2005, *PASP*, 117, 1049

van den Bergh, S., & Mackey, A. D. 2004, MNRAS, 354, 713

Table 1. Observed properties of ten globular clusters in the halo of M31

Identifier ^a	RA (J2000.0)	Dec (J2000.0)	R_p (kpc)	$(m - M)_0$	$E(B - V)$ (meas.)	$E(B - V)$ (lit.)	[Fe/H]	r_h (pc)	M_V	r_{\max} (")
GC1	00 ^h 26 ^m 47 ^s .8	+39°44'45".5	46.4	24.41 ± 0.14	0.09 ± 0.01	0.07	-2.14	3.8	-8.7	20
GC2	00 ^h 29 ^m 44 ^s .9	+41°13'09".8	33.4	24.32 ± 0.14	0.08 ± 0.01	0.07	-1.94	5.2	-7.7	16
GC3	00 ^h 30 ^m 27 ^s .3	+41°36'20".4	31.8	24.37 ± 0.15	0.11 ± 0.01	0.07	-2.14	9.9	-8.5	16
GC4	00 ^h 31 ^m 09 ^s .9	+37°53'59".7	55.2	24.35 ± 0.14	0.09 ± 0.01	0.06	-2.14	6.8	-8.9	20
GC5	00 ^h 35 ^m 59 ^s .7	+35°41'03".6	78.5	24.45 ± 0.15	0.08 ± 0.01	0.07	-1.84	6.3	-8.8	18
GC6	00 ^h 38 ^m 00 ^s .3	+40°43'56".1	14.0	24.49 ± 0.15	0.09 ± 0.01	0.07	-2.14	3.9	-8.4	10
GC7	00 ^h 38 ^m 49 ^s .4	+42°22'48".0	18.2	24.13 ± 0.13	0.06 ± 0.01	0.06	-0.70	7.5	-6.2	10
GC8	00 ^h 54 ^m 25 ^s .0	+39°42'55".5	37.1	24.43 ± 0.14	0.09 ± 0.01	0.05	-1.54	3.2	-8.0	10
GC9	00 ^h 55 ^m 44 ^s .0	+42°46'16".1	38.9	24.22 ± 0.14	0.15 ± 0.01	0.10	-1.54	9.8	-7.2	16
GC10	01 ^h 07 ^m 26 ^s .4	+35°46'49".7	99.9	24.42 ± 0.14	0.09 ± 0.01	0.05	-2.14	4.3	-8.3	20

^aTwo clusters are previously labelled in the literature: GC4 is B514 in Galleti et al. (2005, 2006); GC6 is 298-021 in Barmby et al. (2000).

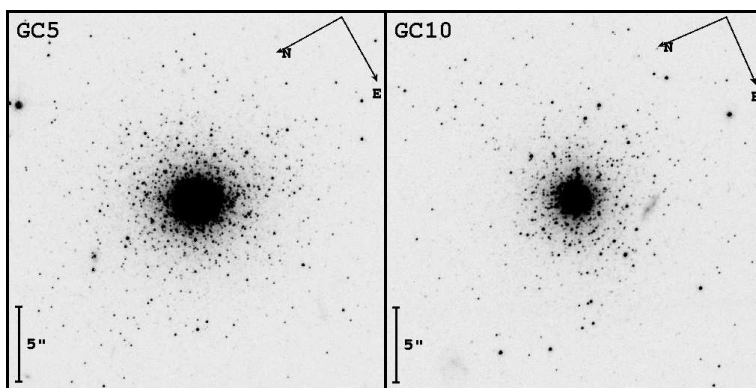
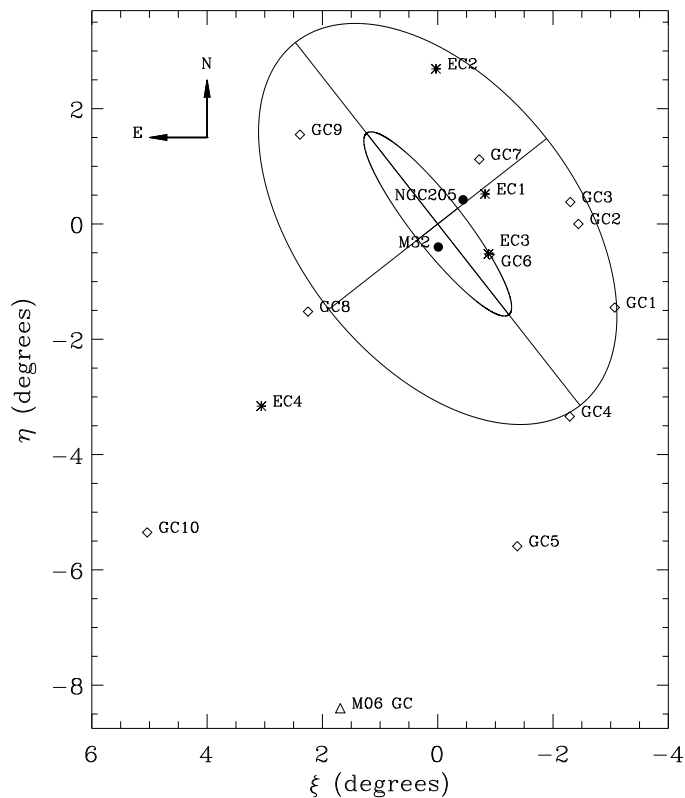


Fig. 1.— The upper panel shows the location of our present cluster sample (open diamonds) in relation to M31. The four luminous, extended clusters from Paper I are marked with stars. Also displayed is the remote cluster of Martin et al. (2006) (open triangle) and two M31 companion galaxies – M32 and NGC 205 (filled circles). The small ellipse delineates the visual extent of the M31 disk. The lower panel shows drizzled ACS/WFC F606W images of the two outermost clusters in our sample ($R_p \sim 78$ and 100 kpc, respectively). Visually, they are representative of the classical globular clusters considered in this paper. Each thumbnail has dimensions of $25'' \times 25''$.

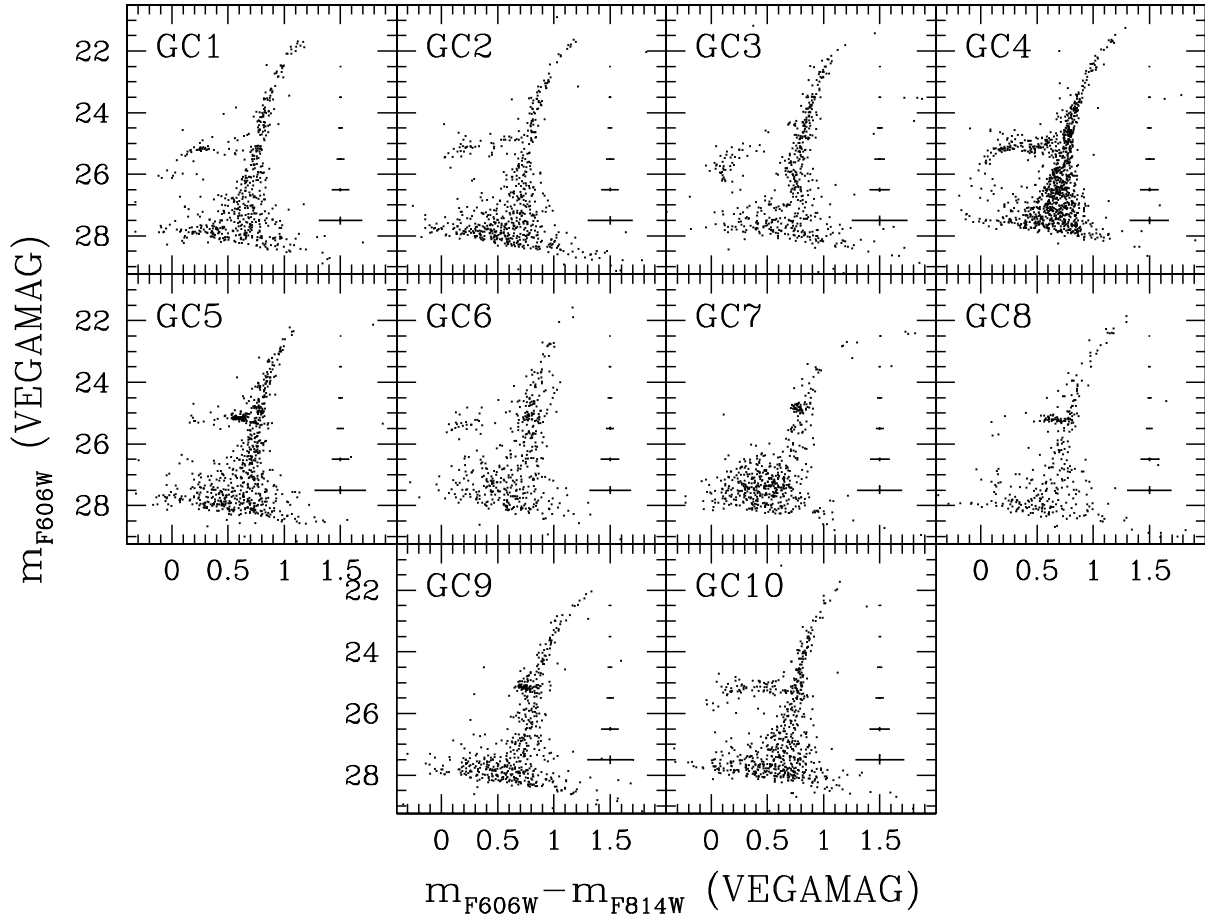


Fig. 2.— CMDs for the ten classical M31 globular clusters. Photometry has been selected from the full ACS/WFC fields by imposing radial limits as described in the text. Typical photometric errors from DOLPHOT are indicated.

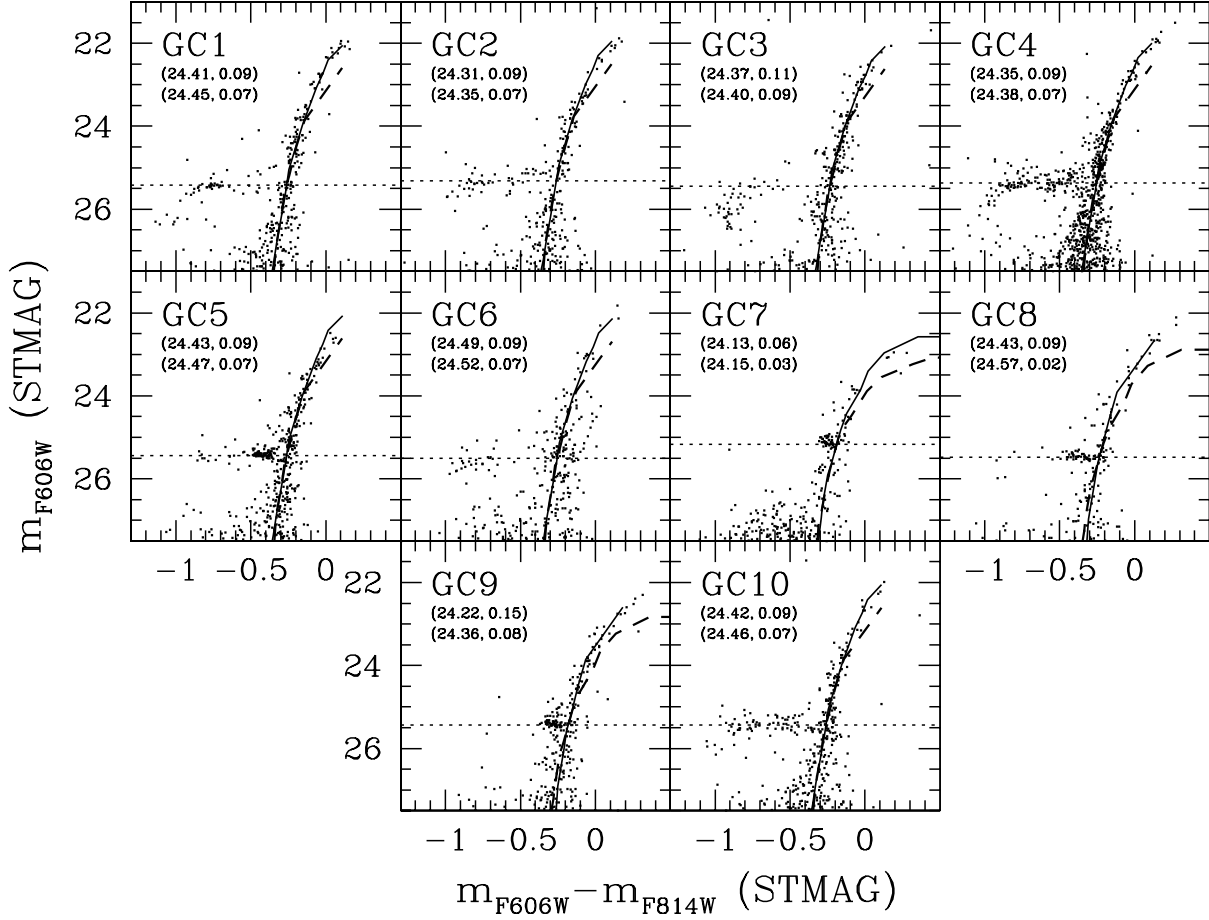


Fig. 3.— Results of fitting the Galactic globular cluster fiducials from Brown et al. (2005) to the observed CMDs. In all panels, the more metal-poor fiducial is marked with a solid line, and the more metal-rich fiducial with a dashed line. The numbers in the upper left of each panel indicate the best fitting $(m - M)_0$ and $E(B - V)$ for the two fiducials – metal-poor above, and metal-rich below. The two marked fiducials for GC7 are 47 Tuc and NGC 5927, which have $[\text{Fe}/\text{H}] = -0.70$ and -0.37 , respectively. For GC8 and GC9 the two fiducials are NGC 6752 ($[\text{Fe}/\text{H}] = -1.54$) and 47 Tuc, while for the remaining seven clusters the two fiducials are M92 ($[\text{Fe}/\text{H}] = -2.14$) and NGC 6752. Photometry has been transformed to STMAG to match the Brown et al. (2005) measurements.